An Eight-Parameter Adaptive Model for the Single Diode Equivalent Circuit Based on the Photovoltaic Module's Physics

Emerson A. Silva, Fabricio Bradaschia, *Member, IEEE*, Marcelo C. Cavalcanti, Aguinaldo Jose Nascimento, Jr., Leandro Michels, *Member, IEEE*, and Luiz Paulo Pietta, Jr.

***Abstract*—This paper proposes an eight-parameter adaptive electrical model based on the physical behavior of the photovoltaic (PV) module with respect to variations of the environmental conditions. In addition, an accurate parameter estimation technique is proposed for this new model based on the pattern search optimization algorithm. The usual characterization of the *I–V* curves has five unknown parameters. The majority of the estimation techniques identify those five parameters for a specific irradiance and temperature. This means that different sets of five parameters are found for each environmental condition, i.e., the estimated parameters are based only on a mathematical fitting with lack of physical meaning. In the proposed eight-parameter adaptive model, it is necessary to execute the parameter estimation technique only once, because the model is valid for all ranges of values of the environmental conditions available on datasheets or experimental curves. Moreover, the restrictions imposed on each parameter make the model capable of emulating the physical behavior of the PV module, particularly useful in fault diagnosis and predictive and corrective maintenance of PV systems. Comparison results based on datasheet and experimental curves are presented to verify the effectiveness of the proposed model and parameter estimation technique.**

***Index Terms*—Adaptive estimation, photovoltaic (PV) cells, PV systems.**

I. Introduction

MATHEMATICAL models for photovoltaic (PV) cell/module are very relevant when a better understanding of its working is necessary. These models have been used to accurately predict the electrical power produced from PV arrays, for simulations of PV arrays under different weather conditions, and for design and optimization of maximum power point (MPP) tracking (MPPT) techniques [1]–[5].

Manuscript received January 25, 2017; revised March 17, 2017; accepted April 27, 2017. Date of publication May 25, 2017; date of current version June 19, 2017. This work was supported in part by the Conselho Nacional de Desenvolvimento Científico e Tecnológico-CNPq, in part by the Coordenação de Aperfeiçoamento de Pessoal de Nível Superior-CAPES, Brazil, and in part by the Fundação de Amparo à Ciência e Tecnologia do Estado de Pernambuco-Facepe, Brazil. *(Corresponding author: Marcelo C. Cavalcanti.)*

E. A. Silva, F. Bradaschia, M. C. Cavalcanti, and A. J. Nascimento, Jr. are with the Department of Electrical Engineering, Federal University of Pernambuco, Recife 50670-901, Brazil (e-mail: emerson.silva90@gmail.com; fabricio.bradaschia@ufpe.br; marcelo.ccavalcanti@ufpe.br; aguinaldojunior10@hotmail.com).

L. Michels and L. P. Pietta, Jr. are with the Power Electronics and Control Research Group, Federal University of Santa Maria, Santa Maria - RS 97105-900, Brazil (e-mail: michels@gepoc.ufsm.br; luizpietta@gmail.com).

Digital Object Identifier 10.1109/JPHOTOV.2017.2703778

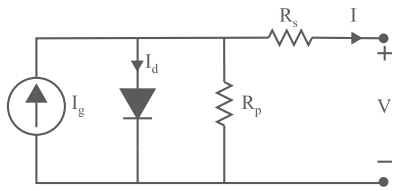

Fig. 1. Equivalent electrical representation of a PV cell.

PV modules present current–voltage (*I–V*) relationships with nonlinear properties that depend on their constructive characteristics as well as of the environmental conditions. Most models for PV cells are based on electrical equivalent circuits that use a set of parameters to represent their *I–V* relationships. The most usual model considers a single-diode approach, which assumes that one lumped diode mechanism is enough to describe the characteristics of the PV cell [6]. Fig. 1 shows the equivalent electrical model of this circuit, which is comprised of a photogenerated current source (I_g), an anti-parallel diode (D), a series resistance (R_s), and a shunt resistance (R_p).

The determination of parameters for the single-diode model of PV cells by analytical techniques [7]–[9] is complex since their *I–V* relationships are described by a set of nonlinear equations whose parameters are reciprocally coupled. Because of this complexity, several different techniques to determine these parameters have been proposed in the literature. Some techniques are based on symbolic evaluation of these equations to determine explicit expressions that give the values of the five parameters [10]–[12]. Techniques based on numerical solutions or iterative algorithm have been also presented [13], [14], where a system of equations is derived for specific operating points provided in datasheets of commercial modules, such as the short-circuit (SC), open-circuit (OC), and MPP operating points. Other approaches to determine the model's parameters apply a curve fitting [15] or optimization algorithms [8], [16]–[22]. These techniques require an *I–V* curve for each PV module, which may be experimental or provided by manufacturers' datasheets.

The major drawback of these techniques is that the determination of the models parameters is only performed at standard test conditions (STC). Consequently, it is required to use an extrapolating method based on PV module's datasheet to determine the parameters for different environmental conditions. As a result, different sets of parameters are obtained for each experimental

I–V curve. Since the estimated parameters are based only on a mathematical fit, there is no physical interpretation for the variation in the parameters. In [23]–[28], equations that relate the variation in the parameters of the PV model with changes in the environmental conditions are proposed, however, with little or no physical validity.

In [15], an estimation technique was proposed to identify the electrical model parameters presenting some correspondence with the physical behavior of PV modules. The technique was able to find five unknown parameters of the single-diode model from data provided by manufacturers' datasheet or experimental curves. The method was based on a full scan of the possible physical values of the parameters at the STC and considered the dependence of R_s on temperature and irradiance. Although interesting, this technique was limited, since it did not consider the other parameters' dependence on temperature and irradiance, i.e., it could not fully represent the physical phenomena of PV modules.

Aiming to solve this limitation, an eight-parameter adaptive model (EPAM) that presents a strict correspondence with the physical behavior of PV modules is proposed in this paper. The model consists of four parameters related to the series resistance R_s ($R_{s,\mathrm{ref1}}$, $R_{s,\mathrm{ref2}}$, k_{Rs}, and γ_{Rs}), three related to the shunt resistance R_p ($R_{p,\mathrm{ref}}$, k_{Rp}, and γ_{Rp}), and one related to the diode ideality factor A (A_{ref}). The other two parameters that describe the behavior of the PV module (I_g and the diode saturation current, I_{sat}) are derived from the previously defined parameters.

The main contribution of this paper is the proposal of an equivalent electrical model for PV modules, where all parameters depend on temperature (*T*) and irradiance (*S*) values, which is a new concept in the literature. Because of the adaptive nature of EPAM, it is necessary to execute the parameter estimation process only once, using a limited set of *I–V* curves acquired for different environmental conditions. The pattern search (PS) was the chosen optimization algorithm in the estimation process of EPAM, because of its well-known capability to obtain high-precision models for PV cells [16], [21]. Although more complex, the resulting eight-parameter model is suitable to determine the behavior of the PV module with accuracy for environmental condition different from the ones used in the parameter estimation process.

The increased complexity of EPAM (when compared with the conventional five-parameter model) is justified by the application areas in which an accurate and flexible electrical model that preserves the physical meaning of the PV modules is necessary.

The model's accuracy is mandatory in areas that need a precise estimation of the PV system generation at specific places. It is possible to use these precise generation data, based on irradiance and temperature annual profiles of a specific location, for choosing the PV module that extracts the most power of a set of available modules; making an optimal design of the PV inverter in terms of efficiency and cost [29]; forecasting the PV system generation to ensure stable and reliable operation of the grid [30]; and calculating the return on investment of the whole PV system in order to attract possible investors.

The flexibility is the capability of the model to extrapolate precise *P–V* and *I–V* curves for irradiance and temperature values different from the ones used in the parameter estimation process. This flexibility is useful when a more reliable and efficient PV system is necessary. For example, it is possible to implement the EPAM in the main controller of a PV inverter in order to [31]: determine the MPP of the PV module at any irradiance and temperature condition, using a precise model-based MPPT algorithm; detect partial shading, dust, or mismatch in PV modules by comparing the real power extracted from the module with the expected power obtained from the model, triggering eventual maintenances.

The connection of the EPAM with the physical phenomena of the PV modules is another important contribution of this paper, embracing application areas like reliability, failure detection, and predictive and corrective maintenance. For example, a set of series resistances (obtained using the proposed EPAM) over time could precisely predict the degradation or aging process of contacts and tracks that connect cells or even a premature failure in the semiconductor junction of a PV cell. Therefore, it is possible to use parameters' tendency curves of a PV module to not only detect the exact moment of failure but also predict failures or premature degradation/aging processes. This is essential for predictive maintenance of PV modules. If a similar procedure is implemented with a PV array with series and parallel connection of modules, it is also possible to detect abrupt changes in the values of series and shunt resistances over time, which could represent failure of a single or group of modules of the array. This is essential for corrective maintenance of modules in a wide PV system [32].

This paper is organized as follows. Section II presents the modeling of the PV cell concerning its physical behavior. Section III describes the EPAM and the proposed parameter estimation technique as well as details of its implementation. Section IV presents simulation and experimental results as well as a comparative analysis. Finally, Section V presents the conclusions of this work.

II. Mathematical Model for Photovoltaic Cells

The equations of the PV module (see Fig. 1) are given by

$$I = I_g - I_{\mathrm{sat}}\left[e^{\left(\frac{V+IR_s}{V_t}\right)} - 1\right] - \frac{V+IR_s}{R_p} \tag{1}$$

$$V_t = \frac{N_s A k T}{q} \tag{2}$$

where V and I are the output voltage and current; V_t is the thermal voltage; q is the electron charge; k is the Boltzmann constant; and T is the temperature; N_s is the number of series-connected cells; I_{sat} is the reverse saturation current; and A is the diode ideality factor.

Usually, it is assumed that only I_g and I_{sat} depend on the environmental conditions, by using [33]:

$$I_g = [I_{g,\mathrm{STC}} + \alpha(T - T_{\mathrm{ref}})]\frac{S}{S_{\mathrm{ref}}} \tag{3}$$

$$I_{\mathrm{sat}} = I_{\mathrm{sat,ref}}\left(\frac{T}{T_{\mathrm{ref}}}\right)^3 exp\left[\frac{qE_g N_s}{kA}\left(\frac{1}{T} - \frac{1}{T_{\mathrm{ref}}}\right)\right] \tag{4}$$

where *S* is the solar irradiation, E_g is the bandgap energy of the solar cell, and α is the temperature coefficient of the SC current. The subscript ref is the value of the parameter at the reference environmental condition. The resistances and A are determined for a reference environmental condition [33]. For other conditions, usually the values found at the reference are repeated or a new estimation process is made. However, to characterize a PV module, it is important to study the dependence on irradiation and temperature of all the parameters of the model.

A. Dependence on Irradiance of Solar Cell Parameters

Throughout its operation, the efficiency of the solar cells is reduced by the dissipation of energy by means of internal resistances. The resistance R_s occurs mainly due to the movement of electrons and the contact metal silicon of the cell [34]. On the other hand, R_p represents parallel high-conductivity paths across the solar cell. These parallel paths are detrimental to the module performance, especially at low irradiances [35].

Therefore, R_s and R_p are important parameters for the PV model. Keeping R_s low is necessary since their growth causes a reduction in power, especially because of a reduction of the SC current [34]. Unlike the R_s, R_p must be high to avoid the reduction of the current in the junction, reducing I_g and the performance of the cell.

Consequently, a special attention is necessary when modeling these parameters, verifying if there are interferences of external factors in their values. Some authors attribute the increase of the conductivity of the active layer with the increase of the irradiance, as one of the reasons for the decrease of R_s. The rate of decrease is faster at low values of *S*, becoming smaller for higher *S* values [36], [37]. This implies $\gamma_{\mathrm{Rs}} < 0$ in

$$R_s(S) = R_{s,\mathrm{ref1}}\left(\frac{S}{S_{\mathrm{ref}}}\right)^{\gamma_{\mathrm{Rs}}} + R_{s,\mathrm{ref2}}. \tag{5}$$

In this paper, this behavior is confirmed through a process of parameter estimation performed in some modules for each one of the curves that represent the module for irradiance variations, provided in their datasheets. Therefore, it results in a power trend line for *T* constant, which is in accordance with some results found in the literature [25], [33], [34].

On the other hand, R_p increases at low irradiance values. Conceptually, R_p is related to the constructive characteristics of the p-n junction. Thereby, a concentration of traps, present in the regions of localized defects, act as collector for photogenerated minority charge carriers. As *S* increases, the traps begin to be filled so that after filling all traps, R_p reaches its maximum value. Thereafter, further increases of *S* at higher levels induce degradation in the PV solar cell, causing the decrease of R_p [34], [37], [38] and consequently implying in $\gamma_{\mathrm{Rp}} < 0$ in

$$R_p(S) = R_{p,\mathrm{ref}}\left(\frac{S}{S_{\mathrm{ref}}}\right)^{\gamma_{\mathrm{Rp}}}. \tag{6}$$

In this paper, this behavior is confirmed through the same process of parameter estimation performed in some modules. As a result of this, it is also possible to express this behavior as a power trend line for *T* constant, which also is in accordance with some results found in the literature [26], [33].

B. Dependence on Temperature of Solar Cell Parameters

When the temperature increases, the maximum power of the cells decreases, especially because of the reduction of the OC voltage [34]. Some studies presented in [39] show that R_s is a thermal-sensitive resistance that belongs to the form of the positive temperature coefficient type. They indicate an exponential or approximately linear growth of R_s with increasing temperature [27], [33], [39]. Arora *et al.* in [36] claim that there is a minimum value for R_s at a particular temperature, and that increasing or decreasing temperature from that point causes R_s to increase. This behavior is explained in terms of the various contributions to the series resistance, such that above room temperature, the sheet resistance of the diffusion layer becomes dominant and R_s increases with temperature, implying $k_{\mathrm{Rs}} > 0$ in

$$R_s(T) = R_{s,\mathrm{ref1}} + R_{s,\mathrm{ref2}}[1 + k_{\mathrm{Rs}}(T - T_{\mathrm{ref}})]. \tag{7}$$

In this paper, this behavior is confirmed through the process of parameter estimation in the previous section, which was repeated, but this time for curves of different temperatures. Though the physical structure of R_s of the cell is complicated, with influence of base contact, base bulk, sheet, and metallic resistances, (7) is a theory equation based on these factors and may accurately predict the values of R_s [39]. A similar conclusion can be found in [27], [33], and [34].

On the other hand, the effect of temperature on R_p is similar to the effect caused by high irradiance. Previous research works report that R_p decreases monotonically with temperature [33], [40]. The rate of decrease is faster at low *T* values exhibiting an approximately linear behavior, especially at temperatures higher than room temperature [27], [40]. This is interpreted as a combination of tunneling and trapping–detrapping of carriers through the defect states that act as recombination centers or traps [41]. From this analysis, it can be inferred that $k_{\mathrm{Rp}} < 0$ in

$$R_p(T) = R_{p,\mathrm{ref}}[1 + k_{Rp}(T - T_{\mathrm{ref}})]. \tag{8}$$

In this paper, this behavior is confirmed through a process of parameter estimation performed in some modules. As result of this, it is possible to express this behavior as a linear trend line for *S* constant. This result also is in accordance with some results found in the literature [27], [34], [41].

III. Proposed Model and Estimation Technique

A. Eight-Parameter Adaptive Model

Based on the studies in the previous section, it is possible to formulate a mathematical EPAM capable of predicting the physical behavior of a PV module. The equations that describe

this model are given by

$$R_s = R_{s,\mathrm{ref}2}[1 + k_{\mathrm{Rs}}(T - T_{\mathrm{ref}})] + R_{s,\mathrm{ref}1}\left(\frac{S}{S_{\mathrm{ref}}}\right)^{\gamma_{\mathrm{Rs}}} \quad (9)$$

$$R_p = R_{p,\mathrm{ref}}[1 + k_{\mathrm{Rp}}(T - T_{\mathrm{ref}})]\left(\frac{S}{S_{\mathrm{ref}}}\right)^{\gamma_{\mathrm{Rp}}} \quad (10)$$

$$A = A_{\mathrm{ref}} \quad (11)$$

$$I_g = I_{\mathrm{SC}}\left(1 + \frac{R_s}{R_p}\right) \quad (12)$$

$$I_{\mathrm{sat}} = \frac{I_g - \frac{V_{\mathrm{OC}}}{R_p}}{e^{\frac{V_{\mathrm{OC}}}{V_t}} - 1}. \quad (13)$$

Equations (9) and (10) include the irradiance and temperature effects simultaneously into R_s and R_p. Piazza and Vitale [28] also considered the two influences simultaneously, but they used purely mathematical expressions without physical foundation. Therefore, the proposed EPAM is the first model to integrate the extrapolation equations of the parameters (as a function of irradiance and temperature) into the optimization algorithm in order to utilize multiple *I–V* curves as input data in the parameter estimation process. Equation (12) is obtained from (1) in the SC condition and represents another way of expressing I_g dependence with S and T. On the other hand, (13) is obtained from (1) in the OC condition and also represents another way of expressing I_{sat} dependence with T.

Finally, according to [42], through the auxiliary expressions

$$I_{\mathrm{SC}} = [I_{\mathrm{SC,ref}} + \alpha(T - T_{\mathrm{ref}})]\left(\frac{S}{S_{\mathrm{ref}}}\right) \quad (14)$$

$$V_{\mathrm{OC}} = V_{\mathrm{OC,ref}} + \beta(T - T_{\mathrm{ref}}) + k_{V\,\mathrm{oc}} V_t \ln\left(\frac{S}{S_{\mathrm{ref}}}\right) \quad (15)$$

where β is the temperature coefficient of the OC voltage, it is possible to estimate I_{SC} and V_{OC} values for any environmental condition so that they can then be applied in (9)–(13).

Although the full model is described by ten parameters, only eight are effectively estimated (hence the name EPAM). These parameters ($R_{s,\mathrm{ref}1}$, $R_{s,\mathrm{ref}2}$, k_{Rs}, γ_{Rs}, $R_{p,\mathrm{ref}}$, k_{Rp}, γ_{Rp}, and A_{ref}) correspond to the intrinsic physical characteristics (form of manufacturing and quality of materials) of the PV module. The remaining two parameters (I_g and I_{sat}) are calculated as a consequence of the other mentioned parameters and only correspond to the PV module operational condition, i.e., a PV module presents different values of I_g and I_{sat} according to the environmental conditions. Then, since N curves representing different values of irradiance and temperature are used, a single value of I_g and I_{sat} is not viable to represent the module. Therefore, the algorithm estimates only eight parameters and I_g and I_{sat} become auxiliary parameters to complete the model.

Therefore, with a set of experimental (or datasheet) curves that encompass relevant ranges of S and T (requiring the use of sensors or estimation techniques to obtain those environmental parameters), it is possible to execute a parameter estimation process for the EPAM. After the estimation process, the resulting EPAM will reproduce the physical behavior of the module, adapting its *I–V* and *P–V* curves according to variations of S and T.

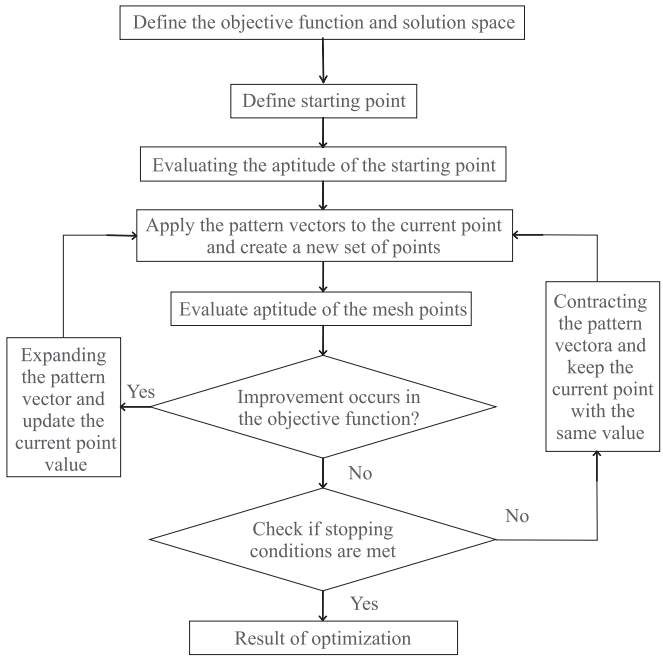

Fig. 2. Flowchart of the PS algorithm [43] used in the proposed parameter estimation technique for the EPAM.

B. Parameter Estimation Technique Based on Pattern Search

To perform the parameters' estimation for the EPAM, some optimization techniques such as genetic algorithm, simulated annealing, and PS were tested, with the PS technique being the one that presented the best results.

The PS algorithm is a multivariate nonlinear global technique capable of solving optimization problems [16]. The PS technique can be explained as follows: it begins by using a set of points, known as a mesh, around the given point [43]. This mesh is made by adding scalar multiple of vectors, called patterns, to the actual point. Subsequently, the algorithm looks for a mesh around the actual point to obtain a point in which the objective function has a lower value; when it happens, this point is defined as the new actual point of the iteration and the mesh dimension becomes larger. Otherwise, the actual point remains the same at the next iteration and the mesh dimension becomes smaller. The stop criteria of the PS technique occur when one of the following cases is reached [43]: the maximum number of iterations; the maximum number of function evaluations; the tolerance on mesh size; tolerance on vector (the distance between two points); or tolerance on function value. The flowchart of optimization using the PS technique is shown in Fig. 2.

The optimization problem is formulated as a minimization of an objective function based on the correlation given in (1), which is used to reduce the value of the mean absolute error in power (MAEP) estimated between the curve originated by the electric model and the curve from the datasheet or from the experimental curve.

The MAEP is based in the error in terms of power:

$$error = |P_{\text{curve}} - P_{\text{model}}| \tag{16}$$

where P_{curve} is the product of V_{curve} and I_{curve} obtained from the datasheet or from the experimental curve, and P_{model} is the product of V_{model} and I_{model} obtained by the simulation of the model with the parameters estimated by the proposed technique.

The MAEP is calculated by

$$MAEP = \frac{\sum_{n=1}^{N_p} error_n}{N_p} \tag{17}$$

where $error$ is calculated for all voltage points going from zero to the OC condition and N_p is the number of voltage points extracted from the datasheet or experimental *I–V* curve of the PV module. This metric, based on *P–V* curves instead of *I–V* curves used on conventional metrics, has already been explored in [15]. The reason for this metric is because most of the applications for the PV electrical model needs accurate values of the generated power. If more than one curve is involved in the estimation process, then a new objective function can be defined by

$$MAEP_{\text{av}} = \frac{\sum_{i=1}^{N_c} MAEP_i}{N_c} \tag{18}$$

where $MAEP_i$ is the individual error of each curve and N_c is the number of curves.

The following is a step-by-step guide to estimate the parameters of the EPAM through the PS algorithm.

1) First, the module constants (k, q, and N_s) are defined.
2) Then, a set of *I–V* (or *P–V*) curves, covering a good variation of irradiation and temperature, is chosen. These are the training curves for EPAM.
3) After that, one of these curves is chosen as a reference (this curve may, for example, represent the average conditions of irradiance and temperature at which the PV module will be subjected) and the PS algorithm (see Fig. 2) is applied to estimate the set [$R_{s,\text{ref}}$, $R_{p,\text{ref}}$, A_{ref}, I_g, I_{sat}] using (17) as the objective function. Besides the starting points vector, two other vectors are defined, representing the lower and upper bounds in which the model parameters are restricted, in order to avoid a parameter to assume values with no physical meaning. The upper bounds (UB), lower bounds (LB), and starting points (X_0) vectors for this estimation process follow the format [$R_{s,\text{ref}}$, $R_{p,\text{ref}}$, A_{ref}] and are defined as
   a) $\text{LB}_1 = [0; 50; 1]$;
   b) $\text{UB}_1 = [3; 10000; 2]$;
   c) $X_{01} = [0.001; 1000; 1]$.
4) Then, the PS algorithm (see Fig. 2) is applied again, now for all available curves (reference and training curves) and under new LB and UB, where (18) is used as the objective function and (9)–(13) are used to form the model. The previous values found $R_{p,\text{ref}}$ and A_{ref} corresponding to the starting points of EPAM. The value found for $R_{s,\text{ref}}$ is divided by two to be used as the starting point of $R_{s,\text{ref1}}$ and $R_{s,\text{ref2}}$. Then, the UB, LB, and X_0 vectors for this estimation process follow the format [γ_{Rs}, γ_{Rp}, k_{Rs}, k_{Rp}, $R_{s,\text{ref1}}$, $R_{s,\text{ref2}}$] and are defined as
   a) $\text{LB}_2 = [-5; -5; 0.001; -0.01; 0; 0]$,
   b) $\text{UB}_2 = [-0.05; -0.05; 0.01; -0.001; R_{s,\text{ref}}; R_{s,\text{ref}}]$,
   c) $X_{02} = (\text{UB}+\text{LB})/2 + \text{LB}$.

   Besides that, the equality constraint

$$R_{s,\text{ref1}} + R_{s,\text{ref2}} = R_{s,\text{ref}} \tag{19}$$

   is employed to ensure consistency with the values obtained in the previous step.
5) The stop criteria used in the PS algorithm were the following.
   a) Maximum number of iterations: 1000.
   b) Maximum number of function (objective) evaluations: 10 000.
   c) Termination tolerance on mesh size, termination tolerance on vector X, and termination tolerance on function value: 2.22×10^{-16}.

IV. Comparison Results

All algorithms presented in this paper are implemented by using MATLAB. In order to evaluate the estimation accuracy of the proposed technique, the MAEP generated for the best set of parameters obtained, in relation to a reference condition, is calculated and compared with the values found for other techniques, already known in the literature, for both types of curves (experimental and datasheets). For the datasheet curves, a curve extractor algorithm developed in MATLAB through image processing was used. For the experimental curves, a curve extractor prototype was developed, including irradiance and temperature sensors together with accurate voltage and current probes to measure the output voltage and current during charging capacitors. In addition, the electrical model generated by each technique is simulated for other environmental conditions, in order to evaluate its performance by means of the average value of MAEP.

A. Datasheet Curves

In this section, the results of the modules SP140PC (a mono crystalline PV module from Shell Solar) and ST40 (a copper indium diselenide-based PV module from Shell Solar) are shown. Table I shows the comparison results, where all parameters were estimated at the reference condition, defined as $S_{\text{ref}} = 1000$ W/m^2 and $T_{\text{ref}} = 25$ °C for both modules. A_{ref} and $R_{p,\text{ref}}$ are the values shown in Table I as A and R_p, respectively.

The remaining parameters found for the EPAM were the following.

1) Module SP140PC:
   $R_{s,\text{ref1}} = R_{s,\text{ref2}} = 0.5\,\text{m}\Omega$;
   $k_{\text{Rs}} = 0.1\%/^\circ\text{C}$;
   $k_{\text{Rp}} = -2.07\%/^\circ\text{C}$;
   $\gamma_{\text{Rs}} = -0.65$;
   $\gamma_{\text{Rp}} = -0.05$.
2) Module ST40:
   $R_{s,\text{ref1}} = R_{s,\text{ref2}} = 247.8\,\text{m}\Omega$;
   $k_{\text{Rs}} = 3.66\%/^\circ\text{C}$;
   $k_{\text{Rp}} = -0.15\%/^\circ\text{C}$;

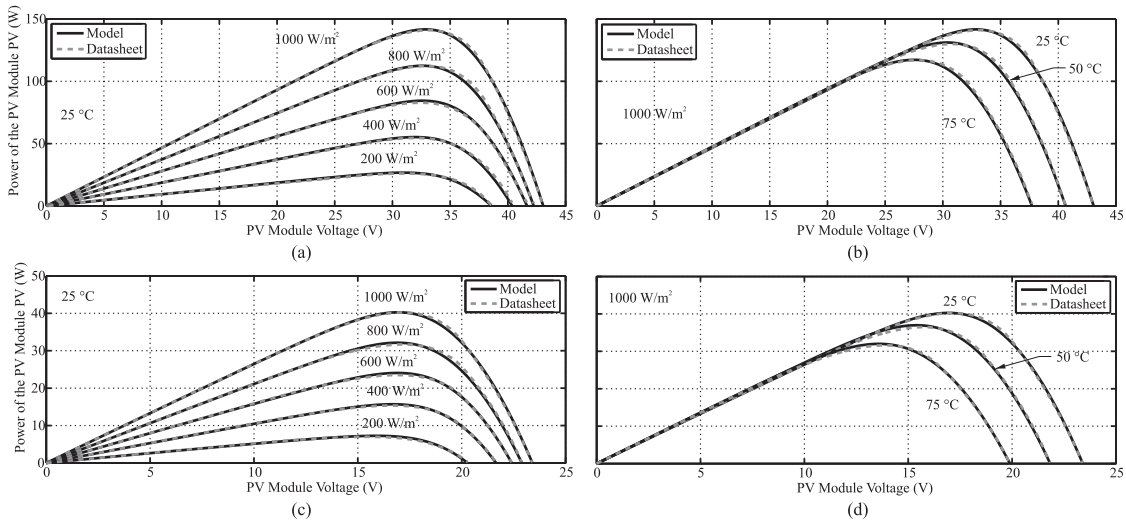

Fig. 3. Comparison between the proposed estimated electrical model and the datasheet curves for the modules (a) and (b) SP140PC and (c) and (d) ST40 at different irradiances and temperatures.

TABLE I
ESTIMATION TECHNIQUES COMPARISON FOR DATASHEET CURVES

Techniques*	A	B	C	D	E
Module SP140PC					
$\mathbf{A}$	1.23	1.16	1.04	1.29	1.02
$\mathbf{R_s(m\Omega)}$	992.6	999.2	999.5	959.0	962.6
$\mathbf{R_p(\Omega)}$	2000.48	797.59	700.67	2828.45	167.89
$\mathbf{I_g(A)}$	4.67	4.65	4.68	4.67	4.70
$\mathbf{I_{sat}(nA)}$	26.59	8.46	1.00	67.08	0.68
Execution Time (s)	400	6	35	478	2
$\mathbf{MAEP_{ref}}(W)$	**0.43**	0.67	0.68	0.45	1.77
$\mathbf{MAEP_{av}}(W)$	**0.50**	0.58	0.96	0.58	1.63
Module ST40					
$\mathbf{A}$	1.57	1.58	1.31	1.59	1.16
$\mathbf{R_s(\Omega)}$	1.21	1.13	3.42	1.21	1.44
$\mathbf{R_p(\Omega)}$	387.72	212.21	1529.40	507.39	174.35
$\mathbf{I_g(A)}$	2.68	2.69	2.66	2.67	2.68
$\mathbf{I_{sat}(nA)}$	616.55	634.42	1.00	741.22	3.36
Execution Time (s)	316	2	34	573	1
$\mathbf{MAEP_{ref}}(W)$	**0.13**	0.22	2.13	0.14	0.60
$\mathbf{MAEP_{av}}(W)$	**0.17**	0.21	2.56	**0.17**	0.36

*Techniques: A - Proposal, B - Nonlinear Least Square [8], C - AlRashidi [16], D - Total Scan [15], E - Accarino [10].

TABLE II
ESTIMATION TECHNIQUES COMPARISON FOR EXPERIMENTAL CURVES

Techniques*	A	B	C	D
Module GBR255				
$\mathbf{A}$	1.33	1.37	1.53	1.33
$\mathbf{R_s(m\Omega)}$	525.8	641.2	459.2	526.0
$\mathbf{R_p(\Omega)}$	238.29	9870.18	77.89	298.80
$\mathbf{I_g(A)}$	9.73	9.85	9.85	9.71
$\mathbf{I_{sat}(\mu A)}$	0.59	1.02	5.05	0.59
Execution Time (s)	122	2	24	35
$\mathbf{MAEP_{ref}}(W)$	**0.98**	5.52	1.34	**0.98**
$\mathbf{MAEP_{av}}(W)$	**0.95**	3.81	2.99	1.00
Module SW130				
$\mathbf{A}$	1.19	1.08	1.00	1.17
$\mathbf{R_s(m\Omega)}$	468.0	526.5	518.1	468.0
$\mathbf{R_p(\Omega)}$	65.46	109.56	50.00	86.51
$\mathbf{I_g(A)}$	8.14	8.12	8.16	8.08
$\mathbf{I_{sat}(nA)}$	58.98	9.03	1.09	63.56
Execution Time (s)	91	1	21	18
$\mathbf{MAEP_{ref}}(W)$	**0.72**	1.63	1.44	0.78
$\mathbf{MAEP_{av}}(W)$	**0.56**	1.56	1.66	0.96

*Techniques: A - Proposal, B - Nonlinear Least Square [8], C - AlRashidi [16], D - Total Scan [15].

$\gamma_{\mathrm{Rs}} = -0.48$;
$\gamma_{\mathrm{Rp}} = -1.45$.

As can be seen in Table I and Fig. 3, the proposed model obtained the best results of the two performance indexes for seven curves at different irradiance and temperature conditions.

B. Experimental Curves

In this section, the results of the modules GBR255 (a poly crystalline PV module from Globo Brasil) and SW130 (a poly crystalline PV module from SolarWorld) are shown. Table II shows the comparison results, where all parameters were estimated at the reference condition, defined as $S_{\mathrm{ref}} = 948$ W/m^2 and $T_{\mathrm{ref}} = 54.5$ °C for the module GBR255 and $S_{\mathrm{ref}} = 913$ W/m^2 and $T_{\mathrm{ref}} = 47.5$ °C for the module SW130. A_{ref} and $R_{p,\mathrm{ref}}$ are the values shown in Table II as A and R_p, respectively. The Accarino technique [10] once again obtained the worst results, and for this reason, it was omitted in the table.

The remaining parameters found for the EPAM were the following.

1) Module GBR255:
$R_{s,\mathrm{ref1}} = R_{s,\mathrm{ref2}} = 262.9$ mΩ;
$k_{\mathrm{Rs}} = 20.73\%/°\mathrm{C}$;

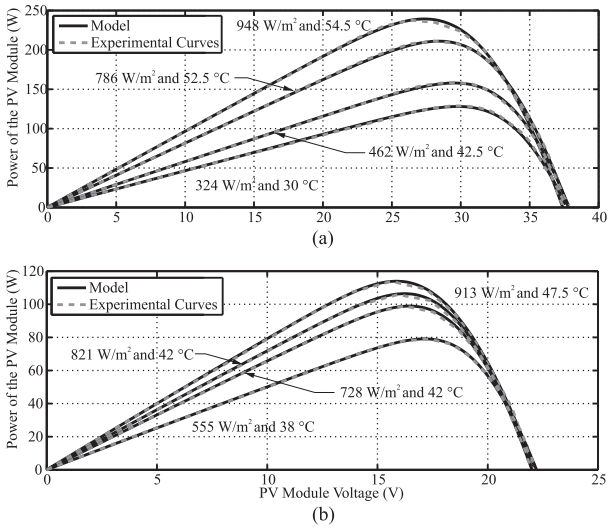

Fig. 4. Comparison between the proposed estimated electrical model and the experimental curves for the modules (a) GBR255 and (b) SW130, at different temperatures and irradiances.

$k_{\mathrm{Rp}} = -0.15\%/^{\circ}\mathrm{C}$;
$\gamma_{\mathrm{Rs}} = -1.7$;
$\gamma_{\mathrm{Rp}} = -0.81$.

2) Module SW130:
$R_{s,\mathrm{ref1}} = R_{s,\mathrm{ref2}} = 234.0\,\mathrm{m}\Omega$;
$k_{\mathrm{Rs}} = 3.9\%/^{\circ}\mathrm{C}$;
$k_{\mathrm{Rp}} = -0.1\%/^{\circ}\mathrm{C}$;
$\gamma_{\mathrm{Rs}} = -0.41$;
$\gamma_{\mathrm{Rp}} = -1.28$.

As can be seen, the proposed model once again obtained the best result of MAEP at the reference condition and the lowest $\mathrm{MAEP_{av}}$ for the four curves at different temperature and irradiance conditions from each PV module. Fig. 4 helps to illustrate that the EPAM can accurately represent the behavior of the experimental curves.

Observing Tables I and II, the proposed EPAM and estimation technique (search algorithm based on the PS) presented the best results in both metrics ($\mathrm{MAEP_{ref}}$ and $\mathrm{MAEP_{av}}$) when compared with four well-known techniques. Although the proposed estimation technique (A) presents the longest execution time, this is not significant because the estimation process needs to be executed only once. The EPAM only needs one set of eight parameters for all possible irradiance and temperature conditions. On the other hand, if techniques B, C, or D are used with the conventional five-parameter model, the estimation process should be executed for every irradiance and temperature combination, leading to large execution times.

Moreover, while the entire parameter estimation process should be done offline, resulting in the values of $R_{s,\mathrm{ref1}}$, $R_{s,\mathrm{ref2}}$, k_{Rs}, γ_{Rs}, $R_{p,\mathrm{ref}}$, k_{Rp}, γ_{Rp}, and A_{ref}, the emulation of the PV module, using the expressions (9)–(13), makes the EPAM capable of operating online in a microcontroller.

Therefore, it can be concluded that the physical behavior of the parameters of the PV module can be described by (9)–(13), resulting in a simple, accurate, and practical model, since it can be applied to more than one environmental condition without the need to run the estimation algorithm more than once, which is different from the techniques that apply the single-diode model. Besides that, the proposed model and technique have shown good versatility, since they can be implemented through curves derived from datasheets or experimental, and they can represent the behavior of several types of PV modules.

V. Conclusion

This paper presented an innovative concept in terms of PV modeling. The proposed model, the EPAM, is based on the physical behavior of the PV module even when variations on the environmental conditions occur. In addition, an accurate parameter estimation technique is proposed for this new model based on the PS optimization algorithm. This new approach presented superior results when compared with well-known techniques, showing that EPAM is effective in emulating the physical behavior of modules, which is particularly useful in fault diagnosis and predictive and corrective maintenance of PV systems.

References

[1] K. J. Sauer, T. Roessler, and C. W. Hansen, "Modeling the irradiance and temperature dependence of photovoltaic modules in PVsyst," *IEEE J. Photovolt.*, vol. 5, no. 1, pp. 152–158, Jan. 2015.

[2] B. Romero *et al.*, "Circuital model validation for s-shaped organic solar cells by means of impedance spectroscopy," *IEEE J. Photovolt.*, vol. 5, no. 1, pp. 234–237, Jan. 2015.

[3] E. Dall'Anese, S. V. Dhople, B. B. Johnson, and G. B. Giannakis, "Optimal dispatch of residential photovoltaic inverters under forecasting uncertainties," *IEEE J. Photovolt.*, vol. 5, no. 1, pp. 350–359, Jan. 2015.

[4] M. Sitbon, J. Leppäaho, T. Suntio, and A. Kuperman, "Dynamics of photovoltaic-generator-interfacing voltage-controlled buck power stage," *IEEE J. Photovolt.*, vol. 5, no. 2, pp. 633–640, Mar. 2015.

[5] K. Rühle, M. K. Juhl, M. D. Abbott, and M. Kasemann, "Evaluating crystalline silicon solar cells at low light intensities using intensity-dependent analysis of I-V parameters," *IEEE J. Photovolt.*, vol. 5, no. 3, pp. 926–931, May 2015.

[6] W. Xiao, F. F. Edwin, G. Spagnuolo, and J. Jatskevich, "Modeling guidelines and a benchmark for power system simulation studies of three-phase single-stage photovoltaic systems," *IEEE J. Photovolt.*, vol. 3, no. 1, pp. 500–508, Jan. 2013.

[7] V. J. Chin, Z. Salam, and K. Ishaque, "Cell modelling and model parameters estimation techniques for photovoltaic simulator application: A review," *Appl. Energy*, vol. 154, pp. 500–519, Sep. 2015.

[8] B. K. Nayak, A. Mohapatra, and K. B. Mohanty, "Parameters estimation of photovoltaic module using nonlinear least square algorithm: A comparative study," in *Proc. IEEE Annu. IEEE India Conf.*, Dec. 2013, pp. 1–6.

[9] S. Shongwe and M. Hanif, "Comparative analysis of different single-diode PV modeling methods," *IEEE J. Photovolt.*, vol. 5, no. 3, pp. 938–946, May 2015.

[10] J. Accarino, G. Petrone, C. A. Ramos-Paja, and G. Spagnuolo, "Symbolic algebra for the calculation of the series and parallel resistances in PV module model," in *Proc. Int. Conf. Clean Elect. Power*, Jun. 2013, pp. 62–66.

[11] E. I. Batzelis, I. A. Routsolias, and S. A. Papathanassiou, "An explicit PV string model based on the lambert W function and simplified MPP expressions for operation under partial shading," *IEEE Trans. Sustain. Energy*, vol. 5, no. 1, pp. 301–312, Jan. 2014.

[12] E. Batzelis and S. Papathanassiou, "A method for the analytical extraction of the single-diode PV model parameters," *IEEE Trans. Sustain. Energy*, vol. 7, no. 2, pp. 504–512, Apr. 2016.

[13] Y. A. Mahmoud, W. Xiao, and H. H. Zeineldin, "A parameterization approach for enhancing PV model accuracy," *IEEE Trans. Ind. Electron.*, vol. 60, no. 12, pp. 5708–5716, Dec. 2013.

[14] C. Carrero, D. Ramírez, J. Rodríguez, and C. Platero, "Accurate and fast convergence method for parameter estimation of PV generators based on three main points of the I-V curve," *Renew. Energy*, vol. 36, pp. 2972–2977, Nov. 2011.

[15] E. A. Silva, F. Bradaschia, M. C. Cavalcanti, and A. J. Nascimento, "Parameter estimation method to improve the accuracy of photovoltaic electrical model," *IEEE J. Photovolt.*, vol. 6, no. 1, pp. 278–285, Jan. 2016.
[16] M. R. AlRashidi, M. F. AlHajri, and A. K. A.-O. K. M. El-Naggar, "A new estimation approach for determining the I–V characteristics of solar cells," *Sol. Energy*, vol. 85, no. 7, pp. 1543–1550, 2011.
[17] J. J. Soon and K. S. Low, "Photovoltaic model identification using particle swarm optimization with inverse barrier constraint," *IEEE Trans. Power Electron.*, vol. 27, no. 9, pp. 3975–3983, Sep. 2012.
[18] K. Ishaque and Z. Salam, "An improved modeling method to determine the model parameters of photovoltaic (PV) modules using differential evolution (DE)," *Sol. Energy*, vol. 85, no. 9, pp. 2349–2359, 2011.
[19] M. P. Cervellini *et al.*, "Optimized parameter extraction method for photovoltaic devices model," *IEEE Latin Amer. Trans.*, vol. 14, no. 4, pp. 1959–1965, Apr. 2016.
[20] N. Rajasekar, N. K. Kumar, and R. Venugopalan, "Bacterial foraging algorithm based solar PV parameter estimation," *Sol. Energy.*, vol. 97, pp. 255–265, Nov. 2013.
[21] M. F. AlHajri, K. M. El-Naggar, M. R. AlRashidi, and A. K. Al-Othman, "Optimal extraction of solar cell parameters using pattern search," *Renew. Energy*, vol. 44, pp. 238–245, Aug. 2012.
[22] F. Bonanno *et al.*, "A radial basis function neural network based approach for the electrical characteristics estimation of a photovoltaic module," *Appl. Energy*, vol. 97, pp. 956–961, Sep. 2012.
[23] J. A. Gow and C. D. Manning, "Development of a photovoltaic array model for use in power-electronics simulation studies," *IEE Elect. Power Appl.*, vol. 146, no. 2, pp. 193–200, Mar. 1999.
[24] W. T. da Costa, J. F. Fardin, D. S. L. Simonetti, and L. de V. B. M. Neto, "Identification of photovoltaic model parameters by differential evolution," in *Proc. IEEE Int. Conf. Ind. Technol.*, Mar. 2010, pp. 931–936.
[25] L. Cerna, V. Benda, and Z. Machacek, "A note on irradiance dependence of photovoltaic cell and module parameters," in *Proc. 28th Int. Conf. Microelectron.*, May 2012, pp. 273–276.
[26] A. Mermoud and T. Lejeune, "Performance assessment of a simulation model for PV modules of any available technology," in *Proc. 25th Eur. Photovolt. Solar Energy Conf. Exhib.*, Sep. 2010, pp. 4786–4791.
[27] S. Bensalem and M. Chegaar, "Thermal behavior of parasitic resistances of polycrystalline silicon solar cells," *Revue Des Energies Renouvelables*, vol. 16, no. 1, pp. 171–176, 2013.
[28] M. C. Di Piazza and G. Vitale, *Photovoltaic Sources Modeling and Emulation*. New York, NY, USA: Springer, 2002.
[29] S. Vighetti, J. P. Ferrieux, and Y. Lembeye, "Optimization and design of a cascaded DC/DC converter devoted to grid-connected photovoltaic systems," *IEEE Trans. Power Electron.*, vol. 27, no. 4, pp. 2018–2027, Apr. 2012.
[30] H. Xin, Y. Liu, Z. Qu, and D. Gan, "Distributed control and generation estimation method for integrating high-density photovoltaic systems," *IEEE Trans. Energy Convers.*, vol. 29, no. 4, pp. 988–996, Dec. 2014.
[31] P. Sharma, S. P. Duttagupta, and V. Agarwal, "A novel approach for maximum power tracking from curved thin-film solar photovoltaic arrays under changing environmental conditions," *IEEE Trans. Ind. Appl.*, vol. 50, no. 6, pp. 4142–4151, Nov./Dec. 2014.
[32] W. Wang *et al.*, "Fault diagnosis of photovoltaic panels using dynamic current-voltage characteristics," *IEEE Trans. Power Electron.*, vol. 31, no. 2, pp. 1588–1599, Feb. 2016.
[33] E. Karatepe, M. Boztepe, and M. Colak, "Neural network based solar cell model," *Energy Convers. Manage.*, vol. 47, nos. 9/10, pp. 1159–1178, 2006.
[34] W. A. El-Basit, A. M. A. El–Maksood, and F. A. E.-M. S. Soliman, "Mathematical model for photovoltaic cells," *Leonardo J. Sci.*, vol. 23, pp. 13–28, 2013.
[35] L. Pan, "Analysis of photovoltaic module resistance characteristics," *Int. J. Eng.*, vol. 26, no. 11, pp. 1369–1376, 2013.
[36] J. D. Arora, A. V. Verma, and M. Bhatnagar, "Variation of series resistance with temperature and illumination level in diffused junction poly- and single-crystalline silicon solar cells," *J. Mater. Sci. Lett.*, vol. 5, no. 12, pp. 1210–1212, 1986.
[37] F. Khan, S.-H. Baek, and J. H. Kim, "Intensity dependency of photovoltaic cell parameters under high illumination conditions: An analysis," *Appl. Energy*, vol. 133, pp. 356–362, 2014.
[38] C.-T. Sah, R. N. Noyce, and W. Shockley, "Carrier generation and recombination in p-n junctions and p-n junction characteristics," *Proc. IRE*, vol. 45, no. 9, pp. 1228–1243, Sep. 1957.
[39] J. Ding, X. Cheng, and T. Fu, "Analysis of series resistance and P-T characteristics of the solar cell," *Vacuum*, vol. 2, no. 77, pp. 163–167, 2005.
[40] K. Nishioka *et al.*, "Analysis of the temperature characteristics in polycrystalline si solar cells using modified equivalent circuit model," *Jpn. J. Appl. Phys.*, vol. 42, no. 12, pp. 71–75, 2003.
[41] E. Cuce, P. M. Cuce, and T. Bali, "An experimental analysis of illumination intensity and temperature dependency of photovoltaic cell parameters," *Appl. Energy*, vol. 111, pp. 374–382, 2013.
[42] F. Lasnier and T. G. Ang, *Photovoltaic Engineering Handbook*. New York, NY, USA: Adam Hilger, 1990.
[43] A. Bagheri and F. Amini, "Control of structures under uniform hazard earthquake excitation via wavelet analysis and pattern search method," *Struct. Control Health Monit.*, vol. 20, pp. 671–685, 2011.

Emerson A. Silva was born in Jaboatão dos Guararapes, Brazil, in 1990. He received the B.Sc. degree in electrical engineering from the University of Pernambuco, Recife, Brazil, in 2012, and the M.Sc. degree in electrical engineering in 2015 from the Federal University of Pernambuco, Recife, where he is currently working toward the Ph.D. degree in electrical engineering.

His primary research interest is in modeling and maximum power point tracking of photovoltaic systems.

Fabricio Bradaschia (S'10–M'13) was born in São Paulo, Brazil, in 1983. He received the B.Sc., M.Sc., and Ph.D. degrees in electrical engineering from the Federal University of Pernambuco, Recife, Brazil, in 2006, 2008, and 2012, respectively.

From August 2008 to August 2009, he worked as a Visiting Scholar with the University of Alcalá, Madrid, Spain. Since October 2013, he is working as an Associate Professor in the Department of Electrical Engineering, Federal University of Pernambuco. His research interests are application of power electronics in photovoltaic systems and power quality, including pulse-width modulation, converter topologies, and grid synchronization methods.

Marcelo C. Cavalcanti was born in Recife, Brazil, in 1972. He received the B.Sc. degree in electrical engineering from the Federal University of Pernambuco, Recife, in 1997, and the M.Sc. and Ph.D. degrees in electrical engineering from the Federal University of Campina Grande, Campina Grande, Brazil, in 1999 and 2003, respectively.

From October 2001 to August 2002, he worked as a Visiting Scholar with the Center for Power Electronics Systems, Virginia Polytechnic Institute and State University, Blacksburg, VA, USA. From September 2012 to August 2013, he worked as a Visiting Scholar at the University of Alcalá, Madrid, Spain. Since 2005, he has been working as an Associate Professor in the Department of Electrical Engineering, Federal University of Pernambuco. His research interests are application of power electronics in photovoltaic systems and power quality, including pulse-width modulation and converter topologies.

Dr. Cavalcanti has been the Editor-in-Chief of the *Brazilian Power Electronics Journal* since January 2016.

Aguinaldo Jose Nascimento, Jr. was born in Recife, Brazil, in 1986. He received the B.Sc. and M.Sc. degrees in physics in 2010 and 2014, respectively, from the Federal Rural University of Pernambuco, Recife, Brazil, where he is currently working toward the Ph.D. degree in electrical engineering.

His primary research interest is in modeling and maximum power point tracking of photovoltaic systems.

Leandro Michels (S'97–M'08) received the B.S. and Ph.D. degrees from the Federal University of Santa Maria, Santa Maria, Brazil, in 2002 and 2006, respectively, both in electrical engineering.

Since 2009, he has been with the Power Electronics and Control Research Group (GEPOC), Federal University of Santa Maria, where he is currently an Adjunct Professor. He has worked in the field of photovoltaic systems as Technical Manager in the laboratory of PV inverters tests, LabEnsaios GEPOC, in working groups to develop Brazilian photovoltaic standards, as well as in R&D projects with industry. His current research interests include photovoltaic systems, modeling and control of static converters, and applied digital control.

Dr. Michels is a Fellow DT-1D of CNPq (technological development and innovative extension).

Luiz Paulo Pietta, Jr. was born in Mucum, Brazil, in 1990. He received the B.Sc. degree in control and automation engineering and the M.Sc. degree in electrical engineering from the Federal University of Santa Maria, Santa Maria, Brazil, in 2014 and 2016, respectively. He is currently working toward the doctoral degree at Grupo de Eletrônica de Potência e Controle (GEPOC), Federal University of Santa Maria.

Since 2010, he has been working at GEPOC. His research interests include photovoltaic systems, industrial networks, power electronics, and digital control.